Pak. J. Chem. 16(3): 150-160, 2026 Research article
ISSN (Print): 2220-2625
ISSN (Online): 2222-307X DOI: 10.15228/2026.v16.i04.p16

Enhancement of Bond Strength Between Polyurethane and Vulcanized Rubber Using Non-Woven Fabric Interlayers for Footwear Soles

Rafaqat Ali[1*] & Sadia Sagar Iqbal[2]
[1] University of Cyprus, Department of Mechanical and Manufacturing Engineering, Panepistimiou Avenue, 2109, Aglantzia, Nicosia, Cyprus
[2]University of the Punjab, Department of Polymer Engineering & Technology, P.O. Box No. 54590, Lahore, Pakistan.
Corresponding Author email: rafaqatalisattar@gmail.com

Abstract
Footwear soles play a critical role in providing protection, comfort, traction, and moisture management under demanding conditions. Inadequate Adhesion between polyurethane midsoles and vulcanized rubber outsoles remains a critical failure mode in high-performance footwear (safety and combat), leading to delamination and reduced service life. Three commercially available non-woven fabrics manufactured in different countries were incorporated into rubber-fabric-PU sandwich structures. Unlike earlier studies that examined rubber-fabric or fabric-PU adhesion in isolation, this work systematically compares three fabrics within an integrated rubber-fabric-polyurethane sandwich architecture, providing new insight into interlayer selection for footwear sole manufacturing. Physical properties, including tensile strength, peel strength, hardness, abrasion resistance, and flex resistance, were evaluated in accordance with relevant ISO standards. Scanning electron microscopy (SEM) and thermogravimetric analysis (TGA) were carried out to investigate thermal stability and interfacial morphology. SEM analysis revealed more continuous rubber penetration and fewer interfacial voids for the German polyester fabric, consistent with its higher peel strength, while the Pakistani polypropylene fabric exhibited higher tensile strength. TGA analysis complemented the SEM findings, confirming that all composites exhibited comparable thermal stability within the operating temperature range. All composites met the requirements of EN ISO 20345:2022 for safety footwear. These findings show appropriate selection of a non-woven fabric interlayer that significantly improves rubber-PU adhesion, offering a viable alternative to chemical treatments and adhesives in high-performance footwear sole manufacturing.

Keywords: vulcanized rubber; polyurethane; non-woven fabric; shoe sole; bonding strength

1. Introduction
The shoe sole is a critical functional component of footwear, acting as the primary interface between the human foot and the ground. It provides load distribution, shock absorption, and biomechanical stability during locomotion. Proper sole design reduces impact-induced injuries and enhances wearer comfort by minimizing stress on joints and soft tissues [1,2].
Elastomeric materials such as natural rubber (NR), styrene-butadiene rubber (SBR), ethylene-propylene-diene monomer (EPDM), and thermoplastic elastomers are widely employed in outsole applications due to their flexibility, abrasion resistance, and energy-dissipation capacity [3–7]. The mechanical performance of these materials is strongly influenced by curing behavior, filler dispersion, and interfacial interactions between polymer chains and reinforcing phases. The incorporation of nano- and micro-scale fillers, including carbon nanotubes and graphene-based materials, has been shown to significantly improve abrasion resistance, tensile strength, and crack propagation resistance in elastomeric systems [8–11].
In footwear composite structures, textile reinforcements play an important role in enhancing structural integrity and load transfer efficiency. Surface modification and functionalization of textile materials have also been reported to improve durability and interfacial performance in composite structures [12]. Interleaving approaches can further enhance through-thickness properties and load transfer in laminated composites [13]. The performance of such hybrid structures is strongly dependent on interfacial adhesion between rubber matrices and textile substrates, which governs delamination resistance and overall durability [2,14–16].
Polyurethane (PU) is widely used in footwear sole systems due to its excellent toughness, flexibility, and energy absorption characteristics. However, the performance of a rubber-PU hybrid system depends on interfacial compatibility, curing conditions, and phase morphology. Poor adhesion between dissimilar polymers can lead to premature failure under cyclic loading. Therefore, controlling interfacial bonding and optimizing composite architecture are essential for improving mechanical reliability and long-term service performance [17–19].
Thermal aging studies on high-performance fabrics have demonstrated significant effects on long-term mechanical durability and service life [20]. In addition, thermal transport behavior in polymer systems is strongly dependent on microstructural design and material composition [21]. Studies on elastomer aging and nanocomposite behavior indicate that filler reinforcement and optimized crosslinking can significantly enhance resistance to thermal degradation and mechanical fatigue [3,22,23].
Standardized mechanical testing methods such as tensile strength, hardness, abrasion resistance, peel strength, and flex resistance are essential for evaluating footwear materials under simulated service conditions [24–28]. These tests provide

quantitative assessment of material performance and enable comparison between different composite systems used in outsole engineering.

This study aims to fabricate rubber-fabric-polyurethane sandwich composites and evaluate their mechanical and thermal performance. The interfacial bonding between the rubber and PU layers is investigated, along with key mechanical properties, including tensile strength, peel/bond strength, hardness, abrasion resistance, and flexural durability. Furthermore, morphological and thermal analyses are conducted to establish structure-property relationships in the developed sandwich composites for potential footwear applications [29–33]. The deformation response of composite materials is also affected by temperature and loading rate, which should be considered when evaluating footwear materials subjected to diverse service environments [34]. Limited attention has been paid to rubber-fabric-polyurethane hybrid structures, particularly those incorporating commercially available nonwoven fabrics as interlayers for footwear applications. The influence of different fabric structures on interfacial bonding behaviour, mechanical performance, and thermal stability in rubber-polyurethane laminate systems has not been systematically investigated.

2.0 Material and Methods

2.1. Rubber

A rubber blend comprising natural rubber (NR), styrene-butadiene rubber (SBR), and polybutadiene rubber (PBR) was used to prepare outsole compounds [35,36]. Ribbed Smoked Sheet grade 3 (RSS-3) natural rubber was imported from Malaysia and selected because of its widespread use in footwear and tire applications. Styrene-butadiene rubber (SBR-1502, TAIPOL, India), containing 23.5 wt.% styrene and 76.5 wt.% butadiene, was incorporated to improve abrasion resistance, tensile properties, fatigue resistance, and heat-aging performance. Polybutadiene rubber (PBR-1220, China) was used to enhance wear resistance, resilience, and wet-traction characteristics.

The rubber formulation also contained zinc oxide and stearic acid as activators, polyethylene glycol (PEG-400) as a processing aid for silica-filled compounds [37], mercaptobenzothiazole disulfide (MBTS), mercaptobenzothiazole (MBT), and tetramethylthiuram disulfide (TMTD) as accelerators [38], sulfur as the vulcanizing agent, and paraffin oil as the processing oil. Carbon black (N330) and precipitated silica were employed as reinforcing fillers. Antioxidants including phenyl-naphthylamine (PBN) and butylated hydroxytoluene (BHT) were incorporated to improve resistance to oxidative degradation [39].

2.1.1. Polyurethane

An ether-based polyurethane (PU) system supplied by Huntsman was used to produce polyurethane midsoles. The PU formulation consisted of isocyanate (SUPRASEC 2444), polyol (DALTOPED FF 55850), catalyst/hardener (DALTOPED FO 00851), and H_2O as blowing agent. The components were processed according to the supplier-recommended reaction injection molding parameters [40,41].

2.1.2. Non-woven Fabric

Rubber-PU sandwiches are made with fabric from three sources. The first fabric was a polyester non-woven fabric purchased from DESMA Schuhmaschinen GmbH, Germany with (gram per square meter) a GSM of 300-350 gm^{-2} and a thickness of 1.21 mm. The second was a polyester non-woven fabric supplied from Enping E-Mart Enterprise Co. Ltd China, with GSM 250-280 gm-2 and a thickness of 1.11 mm. The third fabric was polypropylene purchased from Nayyer Industries (Pvt.) Ltd., Pakistan, with GSM 280-320 gm^{-2} and a thickness of 1.15 mm.

2.1.3. Rubber Compounding

The rubber compound is made in accordance with the formulation [42] as shown in Table 1. The required quantities of natural rubber (NR), styrene-butadiene rubber (SBR), polybutadiene rubber (PBR), fillers, processing aids, curing agents, and other additives were accurately weighed prior to mixing.

Table 1. Compound ingredients for rubber outsole making (Phr: Parts per Hundred Rubber))

Sr.	Component	Function	Phr
1	**RSS-3**	Elastomer	20.0
2	**SBR-1502**	Elastomer	30.0
3	**PBR-1220**	Elastomer	50.0
4	**Rhenosin-260**	Processing aid	2.0
5	**Silica Gel**	Filler	45.0
6	**Carbon Black N330**	Filler	10.0
7	**PEG-400**	Processing aid	3.0
8	**Zinc Oxide**	Activator	4.0
9	**Stearic Acid**	Activator	1.0
10	**PBN / BHT**	Antioxidant	1.0
11	**MBTS**	Accelerator	1.1–1.5
12	**MBT**	Accelerator	0.3–0.5
13	**TMTD**	Accelerator	0.2
14	**Sulfur**	Vulcanizing agent	2.3
15	**Dry Rosin**	Tackifier	0.05
16	**Paraffin Oil**	Plasticizer	10.0

2.1.4. Rubber mixing

The rubber compounds were mixed using a laboratory two-roll mill (Figure 1) at ambient temperature according to established rubber compounding practices [39,43,44]. Mastication of the rubber blend was initially carried out to obtain a uniform plasticity, followed by the sequential incorporation of activators, fillers, processing aids, antioxidants, accelerators, and curing agents. The accelerator system and sulfur were added at the final stage to minimize premature vulcanization [42]. Mixing continued until a homogeneous compound was obtained [39,43,44]. The compounded rubber was then sheeted out to a uniform thickness and conditioned for 24 h prior to molding. Sheets measuring 125 mm × 125 mm were prepared for subsequent compression molding.

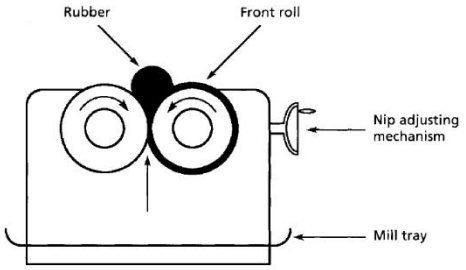

Figure 1. Open mixing mill

2.1.5. Compression Molding

Compression molding was performed using a hydraulic hot press (Figure 2) equipped with electrically heated plates [43]. The mold temperature was maintained at 150 °C [42]. The compounded rubber sheet was placed into the mold cavity, and the selected non-woven fabric was placed and compressed at the top of the mold [42]. After curing, the molded soles with fabrics were removed from the mold, cooled to room temperature, and excess flash was trimmed before further processing.

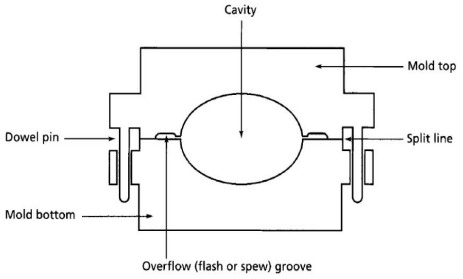

Figure 2. Compressional molding

2.1.6. PU Molding

Polyurethane midsoles were produced using a reaction injection molding process. The polyurethane formulation consists of polyol, isocyanate, catalyst, and water as a blowing agent [45]. Prior to processing, all components were conditioned according to the manufacturer's recommendations to 50-60 °C. The polyol and isocyanate components were mixed at an isocyanate-to-polyol ratio of 72:100 [46] and injected into the mold containing the preformed rubber-fabric composite insert. Polymerization and foaming occurred within the closed mold, resulting in an integrated rubber-fabric-polyurethane structure [47]. The main parts of the machine are shown in Figure 3. The main processing parameters were (Iso and polyol) temperatures of 30-35 °C, mold temperature 45-50 °C, and demold time 4.0 minutes [48]. After demolding, the samples were conditioned at room temperature for at least 72 hours to ensure that post-curing reactions had completed before characterization.

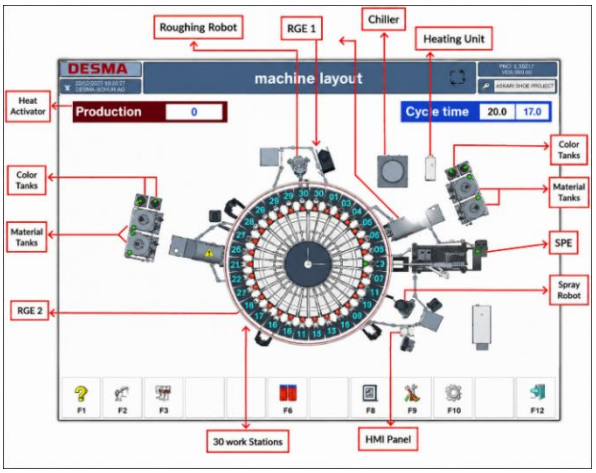

Figure 3. Top view of DESMA machine

2.1.7. Sample Preparation

The fabricated sandwich composites consisted of a vulcanized rubber outsole layer, a non-woven fabric interlayer, and a polyurethane midsole layer (Figure 4). Three commercially available polyester/polypropylene nonwoven fabrics were investigated to assess their effects on interfacial adhesion and mechanical performance. Three samples of each fabric were prepared as test specimens in accordance with the relevant ISO standards for each characterization method [43].

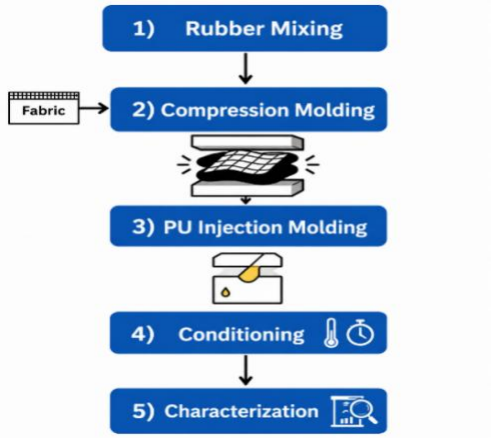

Figure 4. Schematic illustration of the fabrication process

2.2. Characterization

2.2.1. Tensile Properties (ISO 37:2017)

All physical testing required conditioning of the samples in accordance with ASTM D-1610 or ISO 2419. According to these standards, samples were placed 24 hours at 20°C temperature and 65% humidity. The specimens were cut into a dumbbell shape using a die. Width and thickness (mm) of the narrow area of each sample were measured using a vernier caliper and a dead mass thickness gauge, respectively, in accordance with ASTM D-1813.

The specimen was clamped in a tensile testing machine. Jaws separation speed was 350 ± 2 mm/min. Values were recorded in MPa. "HAIDA" China machine (Model HD-B604-S) was used for testing. Gripping was rough to avoid slipping samples. At least 80–85 mm is the breaking gauge length. The breaking force was directly noted from the machine software. Dividing the breaking force by the area of the narrow section of the sample, the ultimate tensile strength was determined [28].

2.2.2. Peel / Bond Strength (ISO 11339:2010)

This technique uses a T-type specimen to determine the peel-off resistance of the bond between two flexible adherents [27]. Two correctly prepared flexible adherents make up laminated test panels (Figure 5). Specially made test panels were 200 mm long and 150 mm wide; however, they were bonded only over approximately 150 mm of the length. Test panels of these same dimensions may also be cut from larger, fully laminated panels.

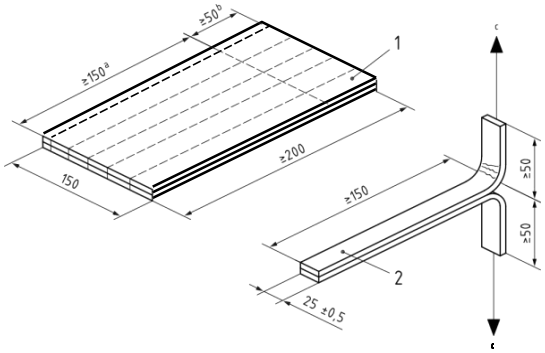

Figure 5. Dimensions of panel samples for the peel strength test [27]

Using a technique that won't be detrimental to the bond, panels were cut into test specimens 25 mm wide. For clamping in the machine's grips, free ends were about 50 mm long and perpendicular to the sample's nip line. Three specimens for each bonding fabric were tested. The tensile machine is identical to the one mentioned in the tensile properties section.

2.2.3. Flex Test (ISO 17707:2005)

A common technique for determining the flex fracture resistance of shoe soles is the sole flex test machine, which is simple in principle and operation. The complete sole was fixed in the jaws of the machine. That method was intended to assess the effect of sole materials and surface patterns on cut growth. An initial cut of 2.0 mm was made at the flexing area [24]. The maximum flex angle was 90° [24]. The control system, in accordance with standard [24], allows programming of the predetermined number of cycles. After completing the cycles, remove the sole and measure the difference in growth between the initial and final cuts.

2.2.4. Abrasion Test (ISO 4649:2010)

The HAIDA International model H-316 abrasion tester is used to evaluate rubber samples. There are two possibilities for this machine: non-rotating (method A) and rotating (method B). Method B was used. Run the reference compound-1 first to determine how much weight it has lost. Weight loss in the range from 180-220 mg [25]. Determine the sample densities, run the samples, and compute the weight loss by deducting the sample's final weight from its initial weight. Express loss in weight/volume. The volume loss was compared with that of the reference compound [25].

2.2.5. Hardness test (ISO 48-4:2018)

Kori Durometer type A (Japan) was used to measure the hardness of rubber as well as PU. According to the standard, the sample thickness must be at least 6.0 mm, and the pressure foot should be at least 12.0 mm from the edge [26]. Place the sample on a solid surface and apply pressure with the durometer until the pressure foot fully contact with the sample's surface. Direct readings were taken from the gauge of the hardness meter.

2.3. Scanning Electron Microscope (SEM)

The morphology of the fabricated composites was investigated using a scanning electron microscope (JSM-6940A, JEOL, Japan). The micrographs were used to evaluate the interfacial characteristics between the rubber, fabric, and polyurethane layers and to assess the extent of mechanical interlocking and adhesion within the composite structure.

3.0. Result and Discussion

A critical challenge in high-performance footwear manufacturing is achieving durable adhesion between polyurethane (PU) midsoles and vulcanized rubber outsoles, as interfacial delamination remains a major cause of premature sole failure [16]. Direct bonding of PU to vulcanized rubber typically requires dedicated bond-strength modeling and surface treatment to achieve reliable adhesion [49], making the process time-consuming and highly formulation-dependent. To address this problem, three commercially available non-woven fabrics were incorporated as an interlayer between the rubber and PU. The resulting rubber-fabric-PU sandwich composites were evaluated using standardized mechanical tests and characterization techniques. The following sections present and compare the results across the three fabric types, with reference to previously reported rubber-fabric and rubber-PU adhesion studies, to identify the best combination of mechanical performance for footwear manufacturing industries.

3.1.1. Tensile Properties

Tensile strength described the primary load-bearing capacity of the composite along the loading axis. It indicates how well the rubber maintained its load-bearing capacity after the addition of fabric and PU. Tensile strength decreased across all sandwich configurations compared with the rubber (Tables 2, 3, and 4). The German fabric composite exhibited the significant reduction, whereas the Pakistani fabric composite showed the lowest (Table 3) [51]. This shows the fabric influences stress transfer across the rubber-fabric-PU interface rather than providing uniform reinforcement. The tensile strengths of the rubber-fabric-PU sandwiches are consistent with values reported for rubber-textile laminates reinforced with woven and knitted fabrics [51], and incorporation of the fabric-PU interlayer does not compromise tensile performance relative to previously reported hybrid rubber laminates [52].

The tensile strength and failure mode of the rubber material are presented in Table 2. The rubber exhibited a tensile strength of 15.33 ± 0.33 MPa, indicating consistent mechanical performance with minimal variation among the tested specimens. During the tensile test, the material failed by breaking, which suggests that fracture occurred once the applied stress exceeded the material's tensile strength. The relatively low standard deviation (±0.33 MPa) demonstrates good repeatability and uniformity in the measured tensile properties. Therefore, improving the rubber-fabric bonding through surface treatments, adhesive optimization, or enhanced curing conditions could further increase tensile strength and overall durability, regardless of fabric origin.

Table 2. Average tensile strength and failure mode of rubber specimens.

Material	Tensile Strength (MPa)	Failure Mode
Rubber	15.33 ± 0.33	Break

Table 3. Tensile properties and failure modes of rubber-fabric sandwich

Fabric Type	Material	Tensile Strength (MPa)	Failure Mode
German Fabric	Rubber-Fabric	10.65 – 10.83	Fabric delamination
Chinese Fabric	Rubber-Fabric	11.45 – 11.57	Fabric delamination
Pakistani Fabric	Rubber-Fabric	10.81 – 11.17	Fabric delamination

Table 4. Tensile properties of rubber-fabric-PU composite

Fabric Type	Tensile Strength (MPa)	Failure Mode
German Fabric	6.01 – 6.23	Fabric delamination
Chinese Fabric	7.22 – 7.46	Fabric delamination
Pakistani Fabric	7.51 – 7.68	Fabric delamination

3.1.2. Peel / Bonding Strength

The required value is 4.0 N/mm according to ISO-20345:2022 [1]. This value was achieved by three fabrics (Table 5). The German fabric showed the strongest adhesion to both rubber and PU, as indicated by its failure mode of fabric than interfacial delamination, consistent with reports of strong mechanical interlocking between polyester-based non-woven fabrics and rubber [16].

Table 5. Peel/bonding performance of rubber-fabric-PU sandwich

Fabric Type	Max Load (N/mm)	Failure Mode
German Fabric	6.61 – 6.84	Fabric break
Chinese Fabric	5.88 – 6.04	Rubber-fabric delaminate
Pakistani Fabric	5.78 – 5.96	Rubber-fabric delaminate

3.1.3. Propagation Peel strength

The Chinese fabric began to propagate at a lower force than the German and Pakistani fabrics (Table 6), indicating a comparatively weak sustained interaction between fabric and PU. Across all three fabrics, propagation peel strength remained below the corresponding maximum peel strength (Figure 6), consistent with the fracture-mechanics view of peel/debonding as a crack that initiates at higher force and then propagates at lower force [51].

Table 6. Propagation peel/bond of rubber-fabric-PU sandwich

Fabric Type	Max Load (N/mm)	Failure Mode
German Fabric	4.43 – 4.78	Fabric break
Chinese Fabric	4.32 – 4.63	Rubber-fabric delaminate
Pakistani Fabric	4.38 – 4.67	Rubber-fabric delaminate

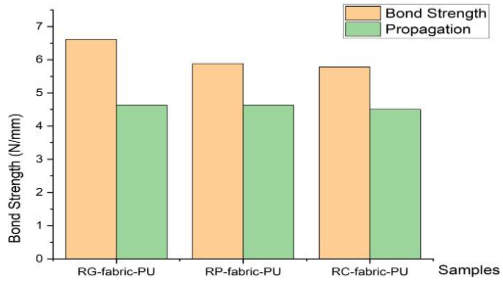

Figure 6. Comparison between Bond & Propagation of Bond strength

3.1.4. Sole Flex Test

The results indicate that fabric type had only a minor effect on cut growth, with the Pakistani fabric composite showing slightly higher cut growth than the German fabric composite (Table 7). Testing was conducted at 45,000 cycles, exceeding the 30,000-cycle requirement specified in EN ISO 20345:2022, and cut growth for all three composites remained at or below the standard (4.0 mm limit) [1] under this higher cycle count, indicating a low probability of sole cracking under normal service conditions.

Table 7. Fatigue cut growth in rubber-based sandwich composites reinforced with different fabric types

Fabric Type	Cycles	Cut Growth (mm)
German Fabric	45,000	3.5 – 3.55
Chinese Fabric	45,000	3.6 – 3.68
Pakistani Fabric	45,000	4.1 – 4.21

3.1.5. Hardness Test

Hardness values of the rubber outsole and PU midsole remained constant in three fabric types (Table 8). The choice of non-woven interlayer exerted a negligible effect on surface hardness. These values are compared with typical ranges reported for footwear-grade vulcanized rubber [35] and microcellular PU [45,47], confirming that incorporation of a fabric interlayer does not compromise the intended hardness of either component.

Table 8. Hardness of outsole and midsole interlayers with fabric in rubber-PU

Fabric Type	Rubber Outsole (Shore A)	PU Midsole (Shore A)
German Fabric	66 – 69	52 – 54
Chinese Fabric	67 – 70	51 – 54
Pakistani Fabric	65 – 68	53 – 55

3.1.6. Abrasion Resistance

Abrasion resistance is a standard test for footwear rubber compound and a major factor in determining outsole service life under repetitive ground contact.

Table 9. Volume loss of rubber outsole material

Material	Abrasion (volume loss mm^3)
Rubber	123.5 – 128.3

The rubber exhibited volume loss, which (Table 9) is within the (EN ISO 20345:2022 requirement of ≤150 mm^3) for outsole materials [1]. This performance is comparable to carbon-black-reinforced NR/EPDM rubber compounds reported in the literature [49], confirming that the outsole's abrasion resistance is adequate for footwear applications. Abrasion resistance was measured on the rubber outsole alone; it is primarily governed by compound formulation and independent of fabric selection.

3.2. Thermal Gravimetric Study

The thermal stability responses of the manufactured laminate composites are shown in Figure 7. The three rubber-fabric-PU sandwich composites were thermally stable up to about 300 °C, and the primary breakdown phase occurred between 300 and 450 °C, a range higher than any temperature encountered during footwear manufacturing or normal service use. The onset temperature and degradation rate were nearly identical among the German, Chinese, and Pakistani fabric composites, indicating that fabric selection has a negligible effect on thermal stability. The main difference was observed only in the final residue: the polyester-based composites (German 33%, Chinese 31-32%) retained a higher residual mass than the polypropylene-based composite 29% [53] due to the chemical structure difference between polyester and polypropylene. So, this is a material-class effect [52,53,54]. So, thermal stability is governed by fabric chemistry. These thermograms support excellent mechanical interlocking as in SEM micrographs [55,56].

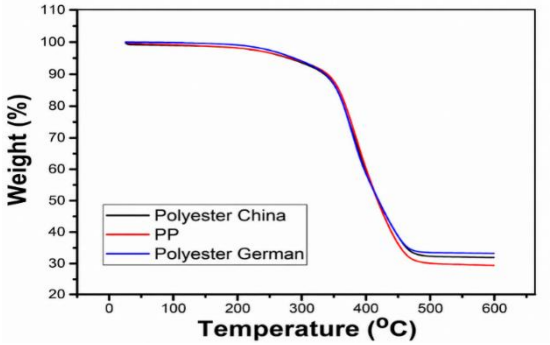

Figure 7. Thermogravimetric curves of RU-Fabric-PU sandwiches with different fabrics

3.3. Scanning Electron Microscope

SEM micrographs of the rubber-fabric-PU sandwich composites are presented in Figure 8 to examine the interfacial morphology among fabric, surrounded by rubber and PU. German and Chinese polyester fabrics (Figure 8a,b), the micrographs reveal a well-defined, continuous interface in which individual fabric fibers are mechanically interlocked with the rubber and PU, with minimal void formation, resulting in the high peel/bond strengths measured. In contrast, Pakistani polypropylene fabric (Figure 8c) exhibits impregnation by rubber and PU; polymers penetrate the fabric structure rather than forming an effective interfacial interlock. Impregnation reduces the effective interfacial area between fibers available for stress transfer and disrupts the structural integrity of the fabric scaffold, thereby limiting the mechanical performance of the composite [57].

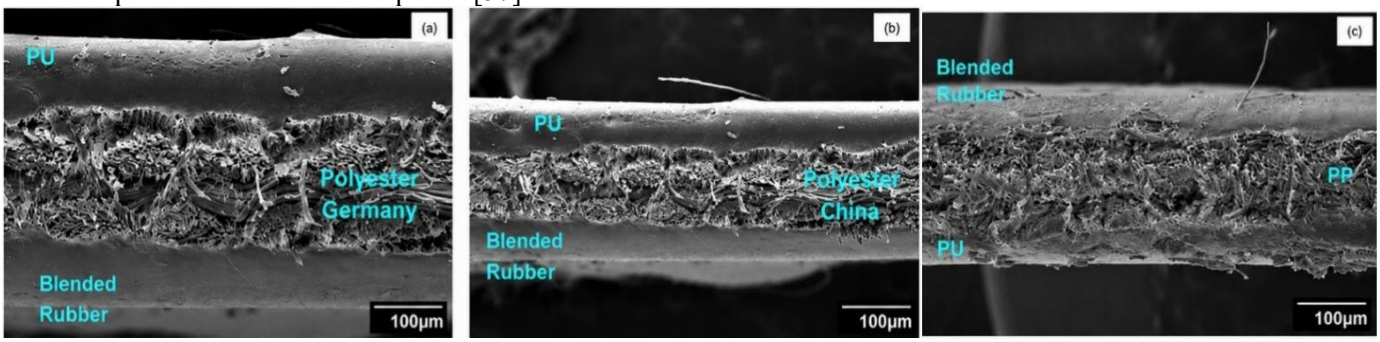

Figure 8. SEM study of RU-Fabric-PU sandwich (a) German fabric, (b) Chinese fabric, (c) Pakistani fabric

4.0 Conclusion

Rubber-fabric-polyurethane sandwich composites were successfully fabricated and systematically evaluated across three commercially available non-woven fabric interlayers to establish structure-property relationships that lead to rubber-PU adhesion in footwear soles. The Pakistani polypropylene fabric yielded the highest tensile strength (7.51-7.68 MPa), whereas the German polyester fabric exhibited significant peel/bond strength (6.61-6.84 N/mm), exceeding the minimum requirement specified by EN ISO 20345:2022 (4.0 N/mm). Importantly, failure was characterized predominantly by

fabric rupture rather than delamination, showing that rubber-fabric-PU interfaces possessed sufficient adhesion to withstand the applied stress and induce cohesive failure within the fabric.

In contrast, hardness, abrasion resistance, and flex fatigue performance were unaffected by fabric type. So, these properties are governed primarily by the rubber and PU formulations, with interlayer fabrics playing a secondary role. SEM and TGA results together show the excellent performance of the German and Chinese fabrics due to mechanical interlocking at the interface. Overall, the results prove that commercially available non-woven fabrics can effectively enhance the adhesion between vulcanized rubber and polyurethane without the use of additional adhesives, a time-consuming process. Among the investigated fabrics, the German polyester non-woven fabric is recommended for applications where interfacial bonding is critical, while the Pakistani polypropylene fabric is preferred for applications requiring higher tensile strength. These findings provide a practical approach for developing durable, high-performance footwear sole systems.

Acknowledgment

We acknowledge experimental support from the Askari shoe project and Firhaj Footwear Pvt Ltd. (Lahore, Pakistan)

Author's Contribution: Rafaqat Ali Writing-original draft, Investigation, Methodology. Sadia Sagar Iqbal (Supervision, writing review & editing, Formal analysis, Resources).

Conflict of Interest: The authors declare no conflicts of interest, financial or personal, that could bias the findings reported here.

Funding Resource: This research was supported by the Askari Shoe Project and Firhaj Footwear (Pakistan). The financial sources had no role in the study design, data analysis, or the decision to publish the results.

References

1. EN ISO 20345:2022 Safety Footwear Standard-Requirements and Test Method
2. Mohammadi, M. M., Nourani, A. (2025). Testing the effects of footwear on biomechanics of human body: A review. Heliyon, 11(4), e42870. https://doi.org/10.1016/j.heliyon.2025.e42870
3. Karekar, A., Schicktanz, C., Tariq, M., Oßwald, K., Reincke, K., Cepus, V., Langer, B., & Saalwächter, K. (2023). Effects of artificial weathering in NR/SBR elastomer blends. Polymer Degradation and Stability, 208, 110267. https://doi.org/10.1016/j.polymdegradstab.2023.110267
4. Costa, N. L., Hiranobe, C. T., Cardim, H. P., Dognani, G., Sanchez, J. C., Carvalho, J. A. J., Torres, G. B., Paim, L. L., Pinto, L. F., Cardim, G. P., Cabrera, F. C., dos Santos, R. J., & Silva, M. J. (2024). A Review of EPDM (Ethylene Propylene Diene Monomer) Rubber-Based Nanocomposites: Properties and Progress. Polymers, 16(12), 1720. https://doi.org/10.3390/polym16121720
5. Bokobza, L. (2023). Elastomer Nanocomposites: Effect of Filler–Matrix and Filler–Filler Interactions. Polymers, 15(13), 2900. https://doi.org/10.3390/polym15132900
6. Bernal-Ortega, P., Bernal, M. M., González-Jiménez, A., Posadas, P., Navarro, R., & Valentín, J. L. (2020). New insight into structure-property relationships of natural rubber and styrene-butadiene rubber nanocomposites filled with MWCNT. Polymer, 201, 122604. https://doi.org/10.1016/j.polymer.2020.122604
7. Roy, K., Debnath, S. C., & Potiyaraj, P. (2019). A critical review on the utilization of various reinforcement modifiers in filled rubber composites. Journal of Elastomers & Plastics, 52(2), 167–193. https://doi.org/10.1177/0095244319835869
8. Vishvanathperumal, S., Roy, J. V., Anand, G., Ramu, K. N., & Praveenkumar, S. (2023). An Investigation on the Effect of the Surface Modifications and HNTs Loading on the Cure behaviours, Abrasion Resistance, Mechanical and Morphological Properties of NR/EPDM Nanocomposites. Silicon, 16(5), 2267–2284. https://doi.org/10.1007/s12633-023-02837-1
9. Tarannum, F., Muthaiah, R., Danayat, S., Foley, K., Annam, R. S., Walters, K. B., & Garg, J. (2022). Chemically Edge-Carboxylated Graphene Enhances the Thermal Conductivity of Polyetherimide–Graphene Nanocomposites. ACS Applied Materials & Interfaces, 14(12), 14753–14763. https://doi.org/10.1021/acsami.1c25279
10. Kumar, V., Lin, W., Wang, Y., Spencer, R., Saha, S., Park, C., Yeole, P., Hmeidat, N. S., Herring, C., Rencheck, M. L., Pokkalla, D. K., Hassen, A. A., Theodore, M., Vaidya, U., & Kunc, V. (2023). Enhanced through-thickness electrical conductivity and lightning strike damage response of interleaved vertically aligned short carbon fiber composites. Composites Part B: Engineering, 253, 110535. https://doi.org/10.1016/j.compositesb.2023.110535
11. De Falco, A., Marzocca, A. J., Corcuera, M. A., Eceiza, A., Mondragon, I., Rubiolo, G. H., & Goyanes, S. (2009). Accelerator adsorption onto carbon nanotubes surface affects the vulcanization process of styrene–butadiene rubber composites. Journal of Applied Polymer Science, 113(5), 2851–2857. https://doi.org/10.1002/app.30261
12. Nasirzadeh, N., Monazam Esmaeelpour, M., Naseri, N., & Omari Shekaftik, S. (2023). Improving ultraviolet protection properties of cotton textiles using Zinc oxide (ZnO) nanomaterials: an approach for controlling

occupational and environmental exposures. International Journal of Environmental Health Research, 34(4), 2067–2087. https://doi.org/10.1080/09603123.2023.2211529

13. Hu, D., Liu, X., Liu, W., Li, G., Rudd, C., & Yi, X. (2022). The effects of compaction and interleaving on through-thickness electrical resistance and in-plane mechanical properties for CFRP laminates. Composites Science and Technology, 223, 109441. https://doi.org/10.1016/j.compscitech.2022.109441
14. El Handari, O., Essaket, I., Abdelkbir, H., El Maliki, A., & Boukhriss, A. (2023). Evaluation of air permeability and moisture management properties of jacquards and basic knitted fabrics. The Journal of The Textile Institute, 115(4), 619–631. https://doi.org/10.1080/00405000.2023.2201530
15. Gungor Turkmen, B., Celik, P., Sehit, H., & Bedez Ute, T. (2023). The effects of hollow yarn and fabric structure on permeability and moisture management properties of woven fabrics. The Journal of The Textile Institute, 115(4), 527–534. https://doi.org/10.1080/00405000.2023.2201109
16. Moustafa, H., Lawandy, S. N., Rabee, M., & Zahran, M. A. H. (2020). Effect of green modification of nanoclay on the adhesion behavior of EPDM rubber to polyester fabric. International Journal of Adhesion and Adhesives, 100, 102617. https://doi.org/10.1016/j.ijadhadh.2020.102617
17. Jørgensen, J. K., Maes, V. K., Mikkelsen, L. P., & Andersen, T. L. (2024). A Precise Prediction of the Chemical and Thermal Shrinkage during Curing of an Epoxy Resin. Polymers, 16(17), 2435. https://doi.org/10.3390/polym16172435
18. Wang, B., Fan, S., Chen, J., Yang, W., Liu, W., & Li, Y. (2023). A review on prediction and control of curing process-induced deformation of continuous fiber-reinforced thermosetting composite structures. Composites Part A: Applied Science and Manufacturing, 165, 107321. https://doi.org/10.1016/j.compositesa.2022.107321
19. Meng, X., Li, Y., AlMasoud, N., Wang, W., Alomar, T. S., Li, J., Ye, X., Algadi, H., Seok, I., Li, H., Xu, B. B., Lu, N., El-Bahy, Z. M., & Guo, Z. (2023). Compatibilizing and toughening blends of recycled acrylonitrile-butadiene-styrene/recycled high impact polystyrene blends via styrene-butadiene-glycidyl methacrylate terpolymer. Polymer, 272, 125856. https://doi.org/10.1016/j.polymer.2023.125856
20. Hoque, Md. S., & Dolez, P. I. (2024). Thermal aging of high-performance fabrics used in the outer shell of firefighters' protective clothing. Journal of Applied Polymer Science, 141(28). https://doi.org/10.1002/app.55624
21. Han, J., Ko, Y.-S., Nam, Y., & Lee, C. (2023). Thermally enhanced osmotic power generation from salinity difference. Journal of Membrane Science, 672, 121451. https://doi.org/10.1016/j.memsci.2023.121451
22. Tayefi, M., Eesaee, M., Hassanipour, M., Elkoun, S., David, E., & Nguyen-Tri, P. (2023). Recent progress in the accelerated aging and lifetime prediction of elastomers : A review. Polymer Degradation and Stability, 214, 110379. https://doi.org/10.1016/j.polymdegradstab.2023.110379
23. Xu, Q., Li, Y., Zeng, F., Zhang, Y., Deng, P., & Su, Z. (2022). Improved ablation resistance and thermal insulation performances of polyimide composites by introducing albite/glass powder composition. Polymers and Polymer Composites, 30. https://doi.org/10.1177/09673911221087806
24. ISO 17707:2005 Test methods for outsoles flex resistance
25. ISO 4649:2024 Rubber, vulcanized or thermoplastic-Determination of abrasion resistance using a rotating cylindrical drum device
26. ISO 48-4:2018 Rubber, vulcanized or Thermoplastic-Determination of hardness
27. ISO 11339:2010 Adhesives T-peel test for flexible-to-flexible bonded assemblies
28. ISO 37:2017 Rubber, vulcanized or thermoplastic-Determination of tensile stress-strain properties
29. Nawab, Y., Jacquemin, F., Casari, P., Boyard, N., Borjon-Piron, Y., & Sobotka, V. (2013). Study of variation of thermal expansion coefficients in carbon/epoxy laminated composite plates. Composites Part B: Engineering, 50, 144–149. https://doi.org/10.1016/j.compositesb.2013.02.002
30. Zhao, D. L., Zhao, Q., & Chung, T.-S. (2021). Fabrication of defect-free thin-film nanocomposite (TFN) membranes for reverse osmosis desalination. Desalination, 516, 115230. https://doi.org/10.1016/j.desal.2021.115230
31. Li, G., Li, H., Wang, G., & Han, C. (2024). Interlaminar performance of three nanomaterials film enhanced glass fiber reinforced polymer. Journal of Reinforced Plastics and Composites, 44(19–20), 1632–1644. https://doi.org/10.1177/07316844241244846
32. Umair, M., Ullah, T., Abbas, A., Nawab, Y., & Seyam, A.-F. M. (2025). Dynamic Mechanical Performance of 3D Woven Auxetic Reinforced Thermoplastic Composites. Journal of Composites Science, 9(12), 649. https://doi.org/10.3390/jcs9120649
33. Huang, P., Wang, J., Hua, J., & Wang, Z. (2022). Non-isothermal Crystallization Kinetics Behavior of Pure Low-density Polyethylene and Low-density Polyethylene/Styrene-butadiene Rubber Thermoplastic Vulcanizates. Journal of Macromolecular Science, Part B, 61(3), 494–505. https://doi.org/10.1080/00222348.2022.2052463

34. Deka, S., Mozafari, F., & Mallick, A. (2024). A comprehensive experimental and modeling study of the strain rate- and temperature-dependent deformation behavior of bio-degradable Mg-CeO_2 nanocomposites. Composites Part A: Applied Science and Manufacturing, 177, 107936. https://doi.org/10.1016/j.compositesa.2023.107936
35. Salkhi Khasraghi, S., Mousavi, S. R., & Arjmand, M. (2025). Tailoring rubber-based shoe outsole compounds: Impact of blend composition and filler type on slip resistance and tribological performance. *ACS Applied Materials & Interfaces, 17*(38), 54065–54081. https://doi.org/10.1021/acsami.5c12680
36. Jovanović, S., Jovanović, V., Marković, G., Samaržija-Jovanović, S., Milićević, Z., Marinović-Cincović, M., & Budinski-Simendić, J. (2019). Elastomers based on NR/BR/SBR ternary rubber blend: Morphological, mechanical and thermal properties. *Chemical Industry and Chemical Engineering Quarterly, 25*(1), 31–38. https://doi.org/10.2298/CICEQ171106016J
37. Huabcharoen, P., Wimolmala, E., Markpin, T., & Sombatsompop, N. (2017). Purification and characterization of silica from sugarcane bagasse ash as a reinforcing filler in natural rubber composites. *BioResources, 12*(1), 1228–1245. https://doi.org/10.15376/biores.12.1.1228-1245
38. Ghosh, P., Katare, S., Patkar, P., Caruthers, J. M., Venkatasubramanian, V., & Walker, K. A. (2003). Sulfur vulcanization of natural rubber for benzothiazole accelerated formulations: From reaction mechanisms to a rational kinetic model. *Rubber Chemistry and Technology, 76*(3), 592–693. https://doi.org/10.5254/1.3547762
39. Rodgers, B. (Ed.). (2015). Rubber Compounding. CRC Press. https://doi.org/10.1201/b18931
40. Prisacariu, C. (2011). *Polyurethane elastomers: From morphology to mechanical aspects*. Springer.
41. Wu, S., Ma, S., Zhang, Q., & Yang, C. (2025). A comprehensive review of polyurethane: Properties, applications and future perspectives. *Polymer, 327*, 128361. https://doi.org/10.1016/j.polymer.2025.128361
42. Ciesielski, A. (1999). *An introduction to rubber technology*. Rapra Technology Ltd.
43. (n.d.). Practice for Rubber-Materials, Equipment, and Procedures for Mixing Standard Compounds and Preparing Standard Vulcanized Sheets. ASTM International. https://doi.org/10.1520/d3182-21ar25
44. The Science and Technology of Rubber. (2013). Elsevier. https://doi.org/10.1016/c2011-0-05820-9
45. Prisacariu, C. (2011). Polyurethane Elastomers. Springer Vienna. https://doi.org/10.1007/978-3-7091-0514-6
46. Mohamed, D. J., Hadi, N. J., & Alobad, Z. K. (2021). Investigation of the Polyol Types and Isocyanate Concentrations on the Rheological, Morphological and Mechanical Properties of Polyurethane Foams. IOP Conference Series: Materials Science and Engineering, 1094(1), 012157. https://doi.org/10.1088/1757-899x/1094/1/012157
47. Kamińska, K., Barczewski, M., Kurańska, M., Malewska, E., Polaczek, K., & Prociak, A. (2022). The Effect of a Chemical Foaming Agent and the Isocyanate Index on the Properties of Open-Cell Polyurethane Foams. Materials, 15(17), 6087. https://doi.org/10.3390/ma15176087
48. Chen, S.-C., Lee, K.-H., Chang, C.-W., Hsu, T.-J., & Feng, C.-T. (2022). Using Gas Counter Pressure and Combined Technologies for Microcellular Injection Molding of Thermoplastic Polyurethane to Achieve High Foaming Qualities and Weight Reduction. Polymers, 14(10), 2017. https://doi.org/10.3390/polym14102017
49. Lee, S.-H., Park, S.-Y., Chung, K.-H., & Jang, K.-S. (2021). Phlogopite-Reinforced Natural Rubber (NR)/Ethylene-Propylene-Diene Monomer Rubber (EPDM) Composites with Aminosilane Compatibilizer. *Polymers, 13*(14), 2318. https://doi.org/10.3390/polym13142318
50. Xu, X., Wang, G., Yan, H., & Yao, X. (2022). Constitutive relationship of fabric rubber composites and its application. Composite Structures, 304, 116302. https://doi.org/10.1016/j.compstruct.2022.116302
51. Bartlett, M. D., Case, S. W., Kinloch, A. J., & Dillard, D. A. (2023). Peel tests for quantifying adhesion and toughness: A review. *Progress in Materials Science, 137*, 101086. https://doi.org/10.1016/j.pmatsci.2023.101086
52. Petkova-Slipets, R., Zlateva, P., & Staneva, D. (2022). Influence of the polyester non-wovens production type on their thermal and flammability properties. *Journal of Engineering and Applied Science, 69*, 51. https://doi.org/10.1186/s44147-022-00107-2
53. Harussani, M. M., Rashid, U., Sapuan, S. M., & Abdan, K. (2021). Low-temperature thermal degradation of disinfected COVID-19 non-woven polypropylene-based isolation gown wastes into carbonaceous char. *Polymers, 13*(22), 3980. https://doi.org/10.3390/polym13223980
54. Risteska, S., Srebrenkoska, V., Zhezhova, S., Srebrenkoska, S., Risteski, S., Jordeva, S., & Golomeova Longurova, S. (2024). The effect of textile structure reinforcement on polymer composite material mechanical behavior. *Polymers, 16*(24), 3478. https://doi.org/10.3390/polym16243478
55. Talaniuk, V., Mistewicz, K., Gawron, A., Marcinkowski, A., Szeluga, U., Myalska-Głowacka, H., Kaja, K. R., Hajra, S., Kim, H. J., & Godzierz, M. (2026). Exploring the potential of multifunctional MWCNT/PDMS nanocomposites in thermal and mechanical energy harvesting. Journal of Thermal Analysis and Calorimetry. https://doi.org/10.1007/s10973-026-15590-5

56. Mi, Q., Yi, S. H., Gang, D. D., Lu, X. G., & Liu, X. L. (2024). Research progress of transpiration cooling for aircraft thermal protection. Applied Thermal Engineering, 236, 121360. https://doi.org/10.1016/j.applthermaleng.2023.121360
57. Teppa, S., & Mears, L. (2009). Bonding Strength Modeling of Polyurethane to Vulcanized Rubber. In SAE Technical Paper Series (Vol. 1). SAE International. SAE World Congress & Exhibition. https://doi.org/10.4271/2009-01-0605

Received: July 04th, 2026 **Accepted: August 10th, 2026**